Combined MRI–PET Scanner: A Monte Carlo Evaluation of the Improvements in PET Resolution Due to the Effects of a Static Homogeneous Magnetic Field

Raymond R. Raylman, Bruce E. Hammer, and Nelson L. Christensen

Abstract—Positron emission tomography (PET) relies upon the detection of photons resulting from the annihilation of positrons emitted by a radiopharmaceutical. The combination of images obtained with PET and magnetic resonance imaging (MRI) have begun to greatly enhance the study of many physiological processes. A combined MRI–PET scanner could alleviate much of the spatial and temporal coregistration difficulties currently encountered in utilizing images from these complementary imaging modalities. In addition, the resolution of the PET scanner could be improved by the effects of the magnetic field. In this computer study, the utilization of a strong static homogeneous magnetic field to increase PET resolution by reducing the effects of positron range and photon noncollinearity was investigated. The results reveal that significant enhancement of resolution can be attained. For example, an approximately 27% increase in resolution is predicted for a PET scanner incorporating a 10-Tesla magnetic field. Most of this gain in resolution is due to magnetic confinement of the emitted positrons. Although the magnetic field does mix some positronium states resulting in slightly less photon noncollinearity, this reduction does not significantly affect resolution. Photon noncollinearity remains as the fundamental limiting factor of large PET scanner resolution.

I. INTRODUCTION

BOTH POSITRON emission tomography (PET) and magnetic resonance imaging (MRI) are diagnostic imaging modalities common to neurology, cardiology, and oncology research. PET's major strength is the ability to visualize and quantify metabolic processes. Although some metabolic imaging is performed with MRI, its main use is in anatomical imaging of soft tissue structures such as the brain. Because of the complimentary nature of these modalities, both PET and MRI find use in characterizing the physiological status of patients. Images from dual studies, however, are difficult to correlate because data from two discrete scanners are necessary. A separate procedure to spatially coregister the image sets must be performed; temporal coregistration is impossible.

With a combined MRI–PET scanner, spatial coregistration is straightforward and temporal coregistration probably could be accomplished. Combining these two modalities into a single scanner would facilitate meaningful comparisons between PET and MRI data. In addition, the combination of these two imaging procedures could improve the in-plane resolution of the PET images due to the effects of a magnetic field on positron transport and the annihilation process.

PET utilizes the coincidence detection of two collinear photons resulting from annihilation of positrons emitted by radiotracers. The physics of positron transport and annihilation ultimately determine the resolution of PET scanners. Upon emission, a positron must lose most of its initial energy before it can annihilate with an electron. Thus, a positron travels some finite distance from its point of origin prior to annihilation. This phenomenon causes the original position of positron emission to be lost, producing a reduction in image resolution. The amount of resolution loss is directly related to the range and, therefore, energy spectrum of positrons emitted by the radionuclide. Derenzo [1] proposed a method to improve resolution by removing the effects of positron range by deconvolving the raw PET data with an appropriate positron range function. Due to the high frequencies present in the positron range function, statistical noise present in the data is amplified, resulting in images with increased noise [2].

If a positron annihilates while there is momentum in the electron–positron system, the resulting photons are not collinear. In order to conserve momentum their angular separation must deviate from 180°; the magnitude of the deviation is mostly dependent upon the amount of momentum. As with the positron range effects, this phenomenon tends to obscure the point of origin of the annihilation event, which causes loss of resolution. Unlike the effect of positron range, however, the effect on resolution due to photon noncollinearity is dependent upon the radius of the PET scanner. The long lever arm inherent in a large scanner tends to amplify the displacement of annihilation events caused by noncollinearity of the annihilation photons. The effect of both of these physical phenomenon on PET scanner resolution can each, to some extent, be reduced by the application of a static magnetic field.

A. Positron Range

Positrons are emitted from proton-rich nuclei. Since the beta decay process involves three particles [proton or neutron, beta particle (positron or electron) and a neutrino (or antineutrino)], the emitted beta particles possess a spectrum of emission energies. These spectra are unique to each radionuclide and can be characterized by the maximum and average energy of the emissions. As beta particles move through matter they continually lose energy in collisions mainly with electrons present in the absorbing material. For the relatively low energy particles emitted in beta decay energy losses due to bremsstrahlung are small. The probability of interaction between a positron and an electron is given by the Bhabha scattering cross section, which is dependent upon the electron density of the absorbing medium and the energy of the positron.

B. Annihilation Photon Noncollinearity

When positrons reach thermal energies two processes can occur: the free positron either forms a bound state with an electron (called positronium) or it annihilates with an electron producing two photons (this type of decay occurs in 64% of the cases [3]). The angular deviations of the photons emitted in free annihilations is approximately 4 mrad [4]. This comparatively large deviation is due to the high momentum of the center of mass in the free positron–electron system. Bound state positronium possesses two ground state configurations: orthopositronium, where the spins of the positron and electron are parallel, and parapositronium, where the spins are antiparallel. One quarter of the bound positrons form parapositronium, whose primary mode of decay is by self-annihilation. In this process the bound particles annihilate with each other. Due to the relatively low energy in the system, the two emitted photons have an angular deviation of approximately 0.5 mrad [5]. In very rare cases the bound positron in parapositronium annihilates with an electron bound to another atom; this results in an angular deviation similar to that produced by free positron annihilation (4 mrad). This mode of annihilation is know as the "pick-off" process. Parapositronium has a mean lifetime of approximately 0.1 ns [6]. Due to conservation of angular momentum, orthopositronium must decay by emission of three photons. Orthopositronium has a much longer lifetime (~100 ns) than does parapositronium. Because of the longer lifetime, many of the positrons in orthopositronium annihilate by the pick-off process before they are able to decay by three-photon self-annihilation. Hence, the majority of positron annihilations result in relatively large angular deviations (either from pick-off or free annihilation events), while only ~17% of the decay events are by self-annihilation [4].

C. Effects of a Magnetic Field

The application of a strong static magnetic field has been proposed as a method for reducing the effects of beta particle range in a wide variety of applications. These uses of magnetic constraint range from enhancement of radiation dose absorbed by tumors [7], [8] to protection of bone marrow during some nuclear medicine procedures [9]. Application of a magnetic field has also been suggested to decrease the loss of resolution of PET scanners caused by positron range effects [4], [10]–[13]. All of these techniques are based upon the fact that a static homogeneous magnetic field exerts a force on a charged particle in motion. This force, known as the magnetic component of the Lorentz force, is given by

$$\vec{F}_{Lor} = q\vec{V} \times \vec{B} \tag{1}$$

where V is the positron's velocity vector, B is the magnetic field vector, and q is the particle's charge. The symbol $\times$ signifies the cross product vector operation. The cross-product nature insures that the magnetic Lorentz force is always directed perpendicular to the particle's path. Consequently, a static magnetic field does not do work on a moving charged particle. Since the force is perpendicular to the magnetic field's direction, the path of the positron curves about the field's axis. A particle moving parallel to the field, therefore, will experience no force. For the most common case of a positron moving at an angle to the axis of the magnetic field, a helical path results. The radius of this helix is given by Enge [14]

$$R = \frac{0.334}{B} \sqrt{(2 \cdot m_p \cdot E_t) + E_t^2} \tag{2}$$

where B is the magnetic field (Tesla, 1T = 10 000 Gauss), m_p is the rest mass of the positron (0.511 MeV), and E_t is the component of the positron's kinetic energy (MeV) perpendicular to the magnetic field. Thus, applying a magnetic field collinear with the axis of the scanner will improve only the in-plane (transaxial) resolution of the PET scanner (Fig. 1).

Application of a magnetic field also affects the noncollinearity of photons emitted by annihilating positrons. The presence of a static magnetic field can mix some of the positronium states. Specifically, the $m_s = 0$ state of orthopositronium (orthopositronium exists in $m_s = \pm 1$ and $m_s = 0$ states) is mixed with the $m_s = 0$ state of parapositronium (parapositronium exists only in the $m_s = 0$ state). It is important to remember that the decay of parapositronium most often results in angular deviations, which are small in comparison to photons emitted from the decay of orthopositronium. Consequently, the number of annihilation events with small photon noncollinearity is increased by the application of a magnetic field. Additional increase in PET resolution may be gained by randomizing the spin states of positronium by application of electromagnetic radiation at the Larmor frequency [which in this application will be in the radio frequency (RF) band]. Thus, an equal amount of ortho- and parapositronium will exist. Given that most emitted positrons (~64%) annihilate before forming positronium, and that approximately 8% of the triplet state positronium decays by self annihilation, an equal population of singlet and triplet state annihilations results in only a ~10% increase in the probability of events that produce photons with small angular noncollinearity compared to the case where just a magnetic field is applied.

In this investigation, we examine the limitations on the resolution of PET scanners imposed by the physics of positron emission and annihilation. Additionally, the application of a magnetic field is explored, by computer simulation, as a means
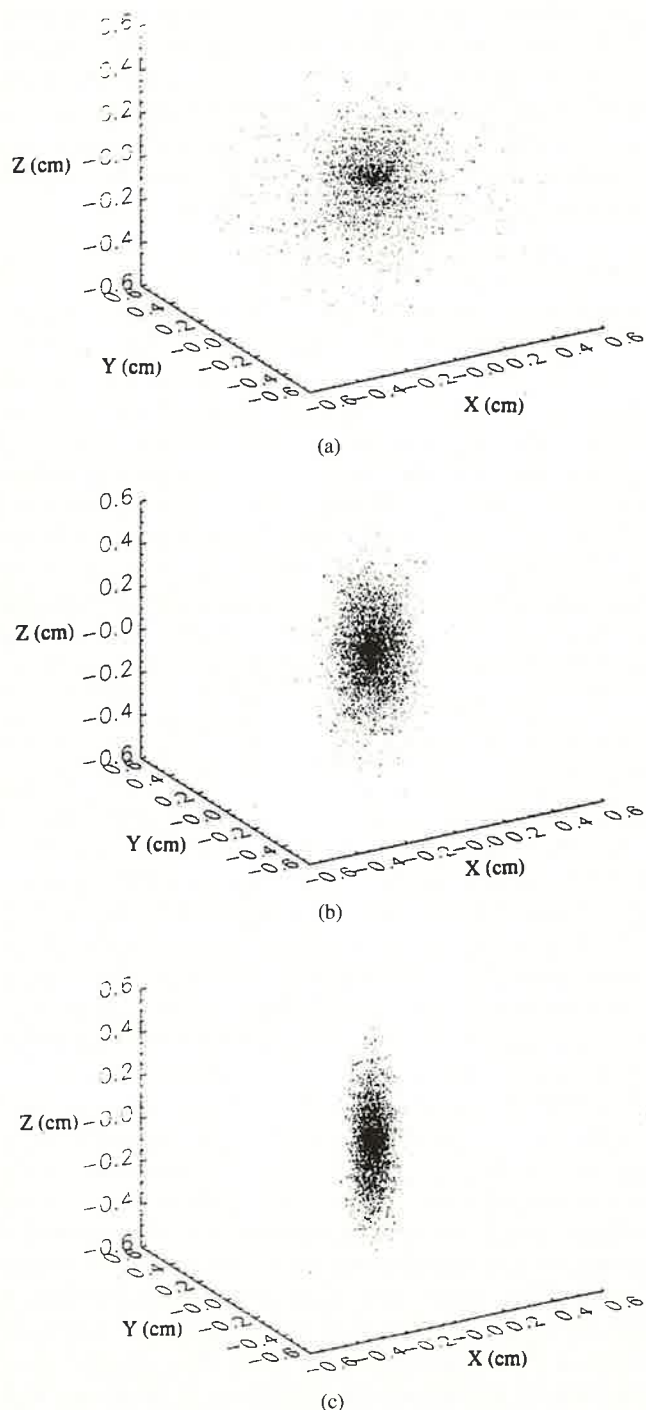
Fig. 1. Three-dimensional distribution of positron end points calculated by the Monte Carlo transport software for a ^{68}Ga point source surrounded by water located at the origin. Plot (a) shows the results for 0 Tesla, plot (b) for 5 Tesla, and plot (c) for 10 Tesla. In all cases the magnetic field is aligned with the z-coordinate axis; thus the particles are magnetically confined in the x–y plane.

Fig. 2. Comparison of point spread functions for a ^{68}Ga point source predicted by the Monte Carlo software (o) with results reported by Hammer *et al.*, (1994) (•). (a) Results for 0 Tesla. (b) Results for 5 Tesla. (c) Results for 9.4 Tesla. The magnetic field was directed perpendicular to the direction of travel of the detectors. Five-centimeter-thick lead blocks with 1 mm × 25 mm slits were used to collimate each of the detectors (CsI coupled to photodiodes). The two coincident detectors were placed 16.4 cm apart.

to enhance resolution beyond these limits. This study extends the previous analysis of Iida *et al.* [10], as we have included all of the effects a strong magnetic field on the resolution of PET scanners from the decrease in positron range to the potential changes in the distribution of the noncollinearity of the annihilation photons. Special attention is paid to the effect of scanner size in systems incorporating magnetic fields in their design.
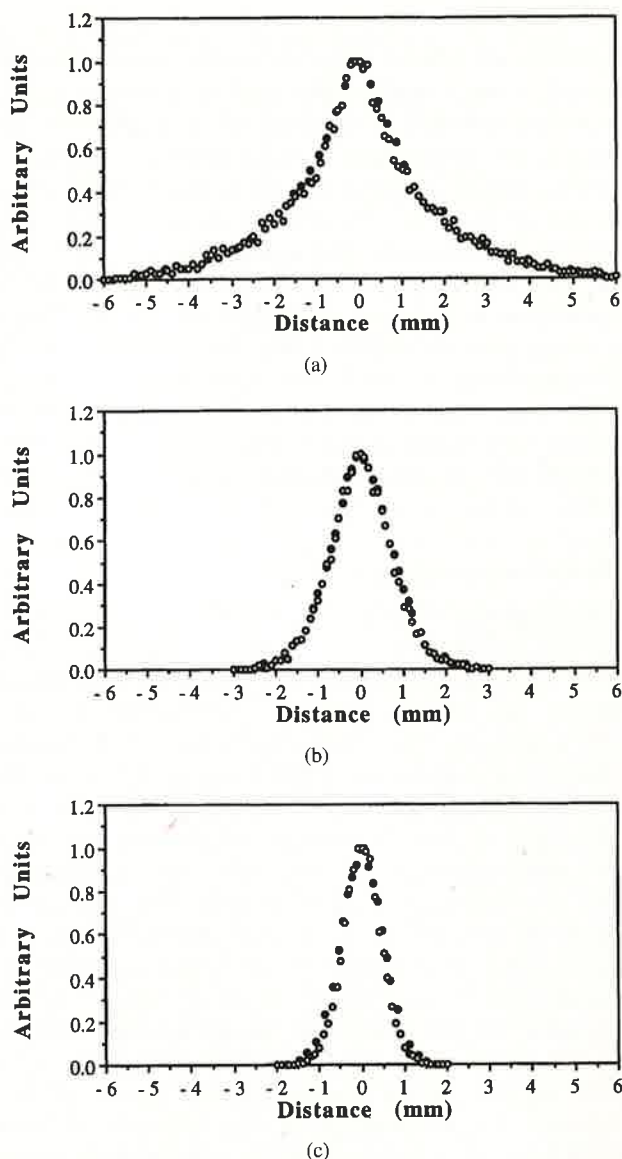
II. MATERIALS AND METHODS

Analysis of the effects of positron emission and annihilation on PET scanner configuration involved two separate Monte Carlo software packages (both developed at the University of Michigan [8], [9]). It was first necessary to simulate the movement of positrons through tissue and the effect of a magnetic field on this motion. This process begins with selection of initial positron energies. Fermi's theory of beta decay [15] was used in conjunction with Von Neumann's rejection method [16] to select positron energies. All emissions were assumed to occur at a single point and the emission directions were taken to be isotropic. The path lengths of each particle was divided into individual segments separated by interaction points. Segment lengths (L) were calculated

using the continuous-slowing-down approximation (CSDA). The energy lost per centimeter of tissue (E_{Loss}) was calculated using the Bethe–Bloch equation [17]. The amount of energy lost by positrons at collision points was estimated by the product of L and E_{Loss}. Histories of secondary electrons (delta rays) were not calculated to reduce computation times. It was assumed that at each interaction point positrons lose energy and are scattered. Scattering angles are assumed to be normally distributed about the origin [18]. The width of this distribution is a function of the energy lost by the particle at the interaction point. When present, the magnetic field was directed along the z-axis of a standard Cartesian coordinate system and aligned with the axis of the scanner. The effect of the magnetic field is added by calculating the angular deflection induced by the Lorentz force (2). Each positron's history was followed until it had lost 99% of its initial energy. Once a particle has lost 99% of its initial energy it has traveled over 99% of its maximum range. Thus, this limit was chosen to aid in reducing computation time without significantly affecting the results. Typically, 100 000 particles were used in each simulation. The end points of individual positrons were stored for future use by the PET scanner simulation software.

Point spread functions (PSF) were created by a very simple simulation program. A pair of square virtual detectors (either 5 mm × 5 mm or 10 mm × 10 mm) in "coincidence" were translated across a simulated positron-emitting point source. Utilizing the end point positions calculated by the positron transport software, the trajectories of emitted annihilation photons were calculated. Given the dimensions and position of a detector pair, it was determined whether the photons struck both detectors (detection efficiency was assumed to be 100%), signaling a coincidence event. In addition, the capability to simulate the presence of a square 10-mm-high lead collimator was included. The collimator was positioned along the sides of the simulated detectors, therefore the length of the collimator was either 5 or 10 mm. Penetration or scattering from the lead was not included in the simulation. Annihilation photon emission angles were randomly selected and the emissions were assumed to be isotropic. A point spread function was created by plotting the number of detected events as a function of detector position. Photon noncollinearity was added by selecting the angle of deviation from an angular noncollinearity distribution measured by Iaci *et al.* [19]. This distribution was modeled with a bi-Gaussian function with narrow and broad components. The narrow Gaussian component models self-annihilation positronium decay events and the broad portion models the larger deviations due to free and pick-off annihilations. Approximately 17% of the events are due to self-annihilation events. Magnetic mixing of states tends to slightly enhance the amount of area under the narrow Gaussian curve with a concomitant decrease in the area under the broader Gaussian. Mixing is saturated at magnetic field strengths above approximately 1.0 Tesla [6]. When a magnetic field is applied, the angular noncollinearity is selected from a single suitably modified distribution (no magnetic field strengths less than 2 Tesla were utilized in this study) calculated from results reported by Iaci *et al.* [19]. The probability of a self-annihilation event occurring
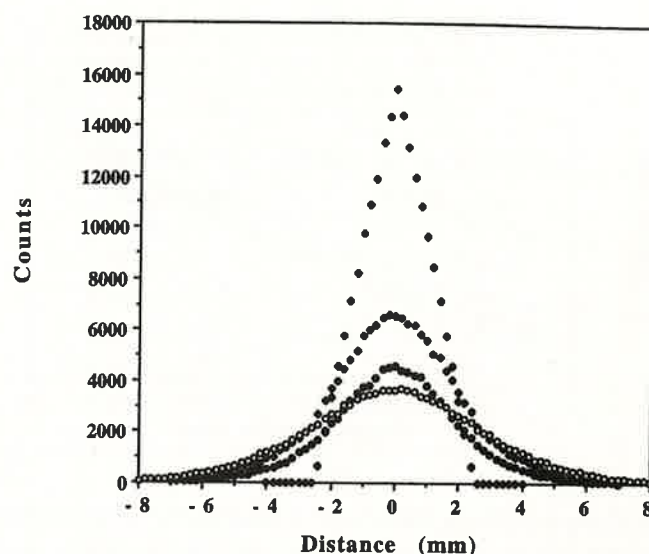

Fig. 3. Demonstration of the smoothing of an ideal point spread function for ^{68}Ga (♦) with a PSF incorporating: annihilation photon noncollinearity (◇), positron range effects (●) and the combination of photon noncollinearity and positron range effects (○). Each detector measured 5 mm × 5 mm and were separated by 100 cm.

increases slightly to approximately 21%. The effect of RF mixing of states was simulated by increasing the probability of self annihilation events from 21–23%, with a concomitantly reduction in the probability of pick-off or free decays. Angular deviation is added to the initial emission angle of one of the photons, either photon can become noncollinear. The resulting PSF's were fit to a Gaussian function; the full width at half maximum (FWHM) of the fit function is reported as the simulated scanner resolution. The effects of Compton scattering were not included in the simulation. Simulated scanner radii ranged from 5–50 cm and magnetic field strengths ranged from 0–15 Tesla.

III. RESULTS

First, the Monte Carlo software's predictions of point spread functions were validated by comparison to results measured at several different magnetic field strengths by Hammer *et al.* [13]. Fig. 2 shows this comparison. The very good agreement between simulated and experimentally determined results indicate that the software was producing reliable predictions of PET scanner resolution with and without the presence of an applied magnetic field. Fig. 3 demonstrates the effect on scanner resolution of positron range and photon noncollinearity. Note that an ideal PSF (no physical effects) measured at the center of the scanner has a triangular shape. This pattern is governed by the solid angle subtended by the point source on to the faces of the detectors. Both physical phenomenon (positron range and photon noncollinearity) act to smooth the ideal PSF, thus reducing resolution.

Fig. 4 demonstrates the increase in resolution of PET cameras (as measured by FWHM of PSF's) produced by application of a magnetic field to a ^{68}Ga (maximum energy = 1.89 MeV) point source. The average reduction in FWHM of point spread functions calculated for 5 mm × 5 mm detectors was approximately 21% and 27% for 5- and 10-Tesla fields,
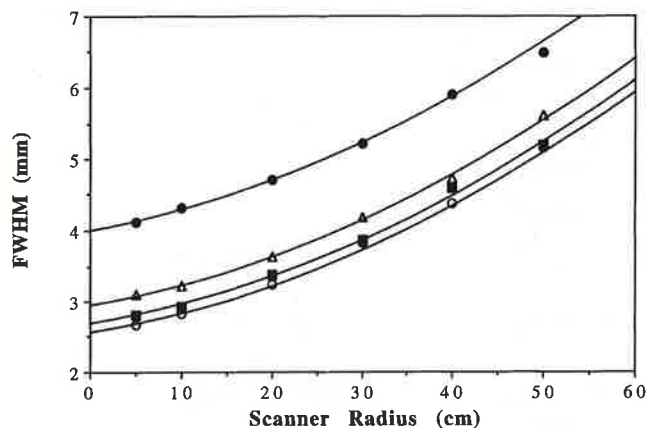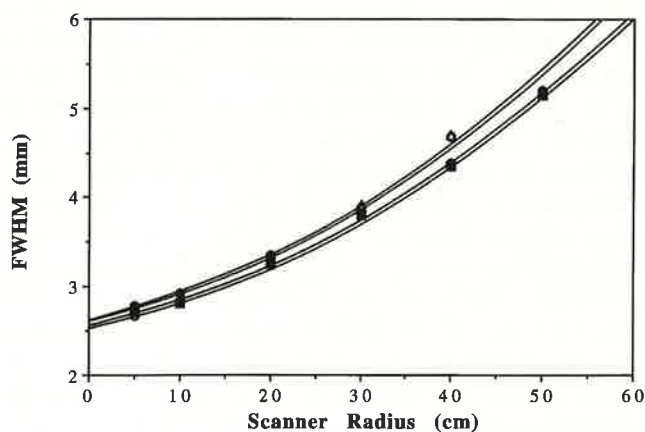
(a)
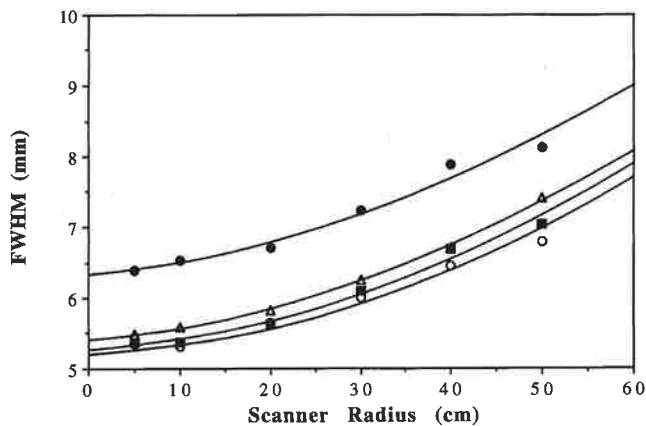
(b)

Fig. 4. Full width at half maximum (FWHM) of a ^{68}Ga point source versus the radius of a simulated PET scanner. The effects of photon noncollinearity at 0 Tesla (o), the combined effects of photon noncollinearity and positron range at 0 Tesla (•), combined effects at 5 Tesla ($\triangle$) and at 10 Tesla (■). (a) Results for 5 mm × 5 mm detectors. (b) Results for 10 mm × 10 mm detectors.

(a)

(b)

Fig. 5. FWHM of a ^{18}F point source versus the radius of a simulated PET scanner. The effects of photon noncollinearity at 0 Tesla (o), the combined effects of photon noncollinearity and positron range at 0 Tesla (•), combined effects at 5 Tesla ($\triangle$) and at 10 Tesla (■). (a) Results for 5 mm × 5 mm detectors. (b) Results for 10 mm × 10 mm detectors.

respectively. For 10 mm × 10 mm detectors, the reductions were ~13% and ~16% at 5 and 10 Tesla, respectively. Fig. 5 displays similar data for an ^{18}F (maximum energy = 0.635 MeV) point source. Average reductions in PSF FWHM for the 5 mm × 5 mm detectors were ~2% and ~3.5% for 5 and 10 Tesla, respectively. In addition, ~0.5% and ~1.5% average reductions in PSF FWHM at 5 and 10 Tesla, respectively, for 10 mm × 10 mm detectors were calculated. Fig. 6 shows a plot of FWHM of a PSF measured with 5 mm × 5 mm detectors versus magnetic field strength for PET scanners with 10- and 30-cm radii. Finally, Table I presents a list of some of the most commonly used PET radionuclides and the maximum energy of their emitted positrons. Note that, as expected, the FWHM was greatest for radionuclides that emit higher energy positrons. Also shown are the effects on resolution of a representative simulated PET scanner when a 10-Tesla magnetic field was applied. The effect of RF mixing on scanner resolution at 10 Tesla is also given.

IV. DISCUSSION

Physical processes inherent in the PET scanning technique ultimately limit the intrinsic resolution of tomographs. Perhaps

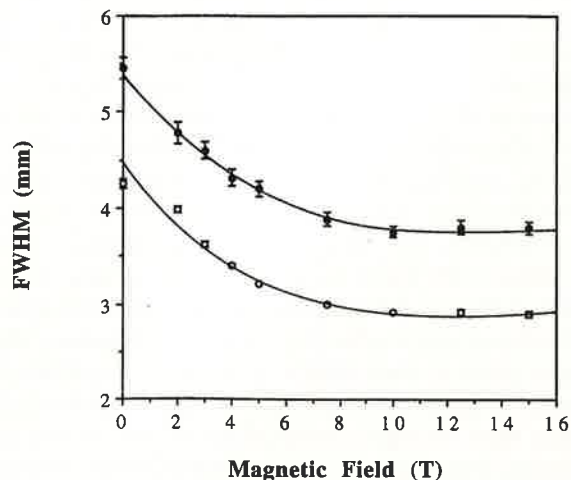Fig. 6. FWHM of PSF (± standard deviation) versus magnetic field strength measured for a ^{68}Ga point source with a 5 mm × 5 mm detector pair. Results for a simulated PET scanner radii of 10 cm (o) and 30 cm (•) are shown.

the most fundamental of these phenomena are effects due to positron transport and annihilation–photon emission. These processes smooth the ideal scanner response, resulting in loss

TABLE I

SOME OF THE MOST COMMON RADIONUCLIDES USED IN PET. SHOWN ARE THE MAXIMUM ENERGY OF THE EMITTED POSITRONS AND THE RESOLUTION (MEAN ± STANDARD DEVIATION) OF A PET SCANNER WITH 0.5 cm × 0.5 cm DETECTORS AND A RADIUS OF 30 cm. ADDITIONALLY, THE EFFECTS OF A 10-TESLA MAGNETIC FIELD AND A 10-TESLA MAGNETIC FIELD PLUS RF MIXING OF POSITRONIUM STATES

Radionuclide	Max. Energy (MeV)	FWHM (0 T) (mm)	FWHM (10 T) (mm)	FWHM (10 T, RF Mix) (mm)
^{11}C	0.96	4.24±0.07	3.85±0.07	3.73±0.07
^{13}N	1.19	4.44±0.06	3.92±0.07	3.80±0.06
^{15}O	1.70	5.28±0.10	3.88±0.07	3.80±0.06
^{18}F	0.64	3.85±0.06	3.78±0.06	3.70±0.06
^{68}Ga	1.89	5.46±0.10	3.90±0.07	3.86±0.06
^{82}Rb	3.15	8.03±0.15	4.13±0.06	3.91±0.05

of resolution. Smoothing of the PSF is illustrated by the plots in Fig. 3. A potentially effective method to reduce these effects is to reduce the range of positrons and noncollinearity of annihilation photons by the application of a strong static homogeneous magnetic field.

The plots in Fig. 4 and data in Table I illustrate that resolution can be significantly enhanced by the application of a strong magnetic field when a high-energy positron-emitting radionuclide (such as ^{68}Ga) is to be utilized. It is also apparent from the results shown in Fig. 4 that blurring caused by annihilation–photon noncollinearity remains virtually unaffected by magnetic mixing of the positronium states. Hence, it is this effect, not positron range, that endures as the most significant limiting factor of PET scanner resolution. In contrast to the data displayed in Fig. 4, the data shown in Fig. 5 for ^{18}F illustrates that very little resolution improvement is achieved by application of a magnetic field. This result is not unexpected, since the average range of positrons emitted from ^{18}F (~1.84 mm) is small relative to positrons emitted by ^{68}Ga (~4 mm) [20].

Both data sets (^{18}F and ^{68}Ga) do, however, share common characteristics from which some significant conclusions can be drawn. First, tomograph resolution is intimately related to the radius of the scanner. This relationship is due mainly to photon noncollinearity. Greater lever arms allow amplification of the blurring effects of photon noncollinearity. Therefore, as noted by many, the ring diameter of PET tomographs plays a major role in determining a scanner's intrinsic resolution limits. These data sets also emphasize the point that a higher relative increase in resolution is obtained by utilizing magnetic confinement in conjunction with high-resolution scanners. For example, with an applied field of 5 Tesla, the PSF FWHM decreases by about 21% for 5 mm × 5 mm detectors, while for 10 mm × 10 mm detectors a 13% decrease is expected. The PSF's of scanners utilizing 10 mm × 10 mm detectors obviously have larger FWHM than those obtained from scanners with 5 mm × 5 mm detectors. Since reduction of positron range is independent of detector size, the relative change in FWHM of the PSF's necessarily become smaller as detector dimensions (and FWHM's) increase. Thus, we expect that even greater gains in resolution are obtainable with scanners with detectors smaller than 5 mm × 5 mm.

This assertion is supported by the results reported by Hammer et al., which showed that FWHM's of a detector pair with 1-mm-wide slits were reduced by ~30% and ~51% at applied magnetic field strengths of 5 T and 10 T, respectively, for a ^{68}Ga point source [13]. It is also important to note that magnetic constraint only occurs in the plane perpendicular to the direction of the magnetic field, as demonstrated by the plots in Fig. 1. Assuming that the magnetic field is collinear with the axis of the PET scanner, we expect, therefore, that only the transaxial resolution will improve, leaving axial resolution virtually unchanged.

Enhancement of annihilation events that produce photons with small angular deviations from 180° by magnetic mixing of positronium states is small. Hence, this effect produced little improvement to PET camera resolution. In addition, the results presented in Table I demonstrate that using RF radiation to induce equal population of positronium states only slightly improves resolution (~3% reduction of PSF FWHM) of a representative PET scanner.

Clearly, magnetic enhancement of PET scanner resolution will be most efficient in high-resolution PET cameras where loss of resolution due to photon noncollinearity is small. Therefore, PET scanners such as those designed for small animal research [21] will benefit most from the effects of magnetic confinement. A strong case for the development of such high-resolution small diameter animal PET scanners to evaluate new pharmaceuticals was made by Hichwa [22]. Indeed, positron range effects are more severe in small animal studies because of the often tiny dimensions of these animals' organs. The effects of positron range has limited the choice of radiopharmaceuticals utilized in animal evaluations to those that are labeled with radionuclides emitting relatively low-energy positrons (e.g., ^{18}F). The use of magnetic constraint could allow the investigation of new radiopharmaceuticals labeled with radionuclides (e. g., ^{11}C and ^{62}Cu) that emit higher-energy positrons. Furthermore, autoradiographic methods using beta-emitting radionuclides may also be improved by the application of magnetic fields. Degradation of resolution from beta range effects could be reduced by the magnetic constraint of these energetic particles. This application has been successfully demonstrated in a preliminary study by Meyer [23].

The results presented in Fig. 6 demonstrate that the reduction of PSF FWHM becomes saturated at high magnetic field strengths. Increasing the magnetic field above approximately 12 Tesla produces relatively small improvements in resolution. Thus, there is a limit upon the field strength desirable for future PET scanners that incorporate magnetic fields. It should be noted that at field strengths below 12 Tesla the improvement in resolution is significant. For example, at 5 Tesla the average intrinsic resolution increases by approximately 21% (for ^{68}Ga). Hence, existing high-field MRI scanners may be effectively utilized to enhance PET scanner resolution.

Possibly the most challenging aspect of designing a MRI–PET scanner will be selection of radiation detection systems that can operate in high-magnetic-field environments. Photomultiplier tubes, which are commonly used to collect and amplify scintillation light, are highly sensitive to the effects of magnetic fields and hence will present difficulties in this application. Therefore, the use of alternative devices such as avalanche photodiodes [12], silicon photodiodes [13], and fiber-optically coupled photomultiplier tubes are being explored. In addition, the effects of RF on signal quality and introduction of field inhomogeneities caused by the presence of the detectors are currently under investigation. The incorporation of a PET scanner with an MRI scanner may prove to be economically unfeasible. Alternatively, a separate removable PET scanner module designed to fit inside a standard MRI machine could be constructed. Therefore, the PET detectors are in the MRI scanner only when needed. This would aid in reducing cost, since the owner of an existing MRI scanner need only acquire the PET module and its associated electronics. The detectors, configuration, and scanning protocols to be used with a combined MRI-PET scanner are subjects of ongoing research and are beyond the scope of this investigation. The ultimate goal, however, is to produce a device that can acquire simultaneous (or near simultaneous) MRI and PET images.

V. CONCLUSION

In conclusion, we have verified that the application of a strong static homogeneous magnetic field can significantly enhance the resolution of PET scanners, especially for high-energy positron-emitting radionuclides and high-resolution scanners. The effect of annihilation photon noncollinearity, however, limits improvements. While the magnetic and RF mixing of quantum states of positronium will reduce the noncollinearity of some annihilation photons, the change is too small to produce a significant improvement of resolution. Therefore, annihilation photon noncollinearity remains as the process that ultimately limits the resolution of large PET scanners. The radius of any future MRI-PET scanner must thus be optimized to enhance the resolution gains achieved by magnetic confinement. In smaller devices, such as those designed for animal studies, magnetic reduction of positron range allows for the broadening of the choice of

radiopharmaceuticals. Possibly the most significant advantage of combining a PET scanner with a magnet is the potential for obtaining near-simultaneous MRI and PET scans. Thus, vastly simplifying the spatial and temporal fusion of data from these two complementary medical imaging modalities. The future of combined MRI-PET machines depends upon the ability to physically combine the necessary hardware and perhaps more importantly the desire to proceed with such a coupling.

REFERENCES

[1] S. E. Derenzo, "Mathematical removal of positron range blurring in high resolution tomography," *IEEE Trans. Nucl. Sci.,* vol. 33, pp. 565–569, 1986.

[2] S. F. Haber, S. E. Derenzo, and D. Uber "Application of mathematical removal of positron range blurring in positron emission tomography," *IEEE Trans. Nucl. Sci.,* vol. 37, pp. 1293–1299, 1990.

[3] P. Colombino and B. Fiscella, "Positronium annihilation in magnetic fields up to 21 kG," *Nuovo Cimento,* vol. 3, pp. 1–14, 1971.

[4] D. W. Rickey, R. Gordon, and W. Huda, "On lifting the inherent limitations of positron emission tomography by using magnetic fields (MagPET)," *Automedica,* vol. 14, pp. 355–369, 1992.

[5] V. I. Goldanskii, "Physical chemistry of the positron and positronium," *Atomic Energy Rev.,* vol. 6, pp. 3–148, 1968.

[6] O. Halpern "Magnetic quenching of the positronium decay," *Phys. Rev.,* vol. 94, pp. 904–907, 1954.

[7] C. C. Shih, "High energy electron radiotherapy in a magnetic field," *Med. Phys.,* vol. 2, pp. 9–13, 1975.

[8] R. R. Raylman and R. L. Wahl, "Magnetically enhanced radionuclide therapy," *J. Nucl. Med.,* vol. 35, pp. 157–163, 1994.

[9] _____, "Magnetically enhanced protection of bone marrow from beta particles emitted by bone-seeking radionuclides: Theory of application," *Med. Phys.,* vol. 22, pp. 1285– 1292, 1995.

[10] H. Iida, S. Kanno, S. Miuri, M. Murakami, K. Takahashi, and K. Uemura, "A simulation study of a method to reduce positron annihilation spread distributions using a strong magnetic field in positron emission tomography," *IEEE Trans. Nucl. Sci.,* vol. 33, pp. 597–600 1986.

[11] B. E. Hammer, "NMR-PET scanner apparatus," U.S. Patent 4 939 464, 1990.

[12] R. R. Raylman, "Reduction of positron range effects by the use of a magnetic field: Use in positron emission tomography," Ph.D. dissertation, Univ. of Michigan, 1991.

[13] B. E. Hammer, N. L. Christensen, and B. G. Heil, "Use of a magnetic field to increase the spatial resolution of positron emission tomography," *Med. Phys.,* vol. 21, pp. 1917– 1920, 1994.

[14] H. Enge, *Introduction to Nuclear Physics,* 2nd ed. Reading, MA: Addison-Wesley, 1966.

[15] R. D. Evans, *The Atomic Nucleus,* 3rd ed. New York: McGraw-Hill, 1977.

[16] S. Ross, *A First Course in Probability,* 2nd ed. New York: Macmillan, 1976.

[17] E. Segré, *Nuclei and Particles,* 2nd ed. Reading, PA: Benjamin/Cummings, 1976.

[18] E. J. Williams, "Electron scattering from thin targets," in *Proc. Royal Acad. Sci.,* 1939, vol. A169, pp. 531–542.

[19] G. Iaci, I. F. Quercia, and E. Turrisi, "Positron annihilation in water and ice with an external magnetic field," *Nuovo Cimento,* vol. 24, pp. 1950–1960, 1962.

[20] Z. H. Cho, J. K. Chan, L. Ericksson, M. Singh, S. Graham, N. S. MacDonald, and Y. Yano, "Positron ranges obtained from biomedically important positron-emitting radionuclides," *J. Nucl. Med.,* vol. 16, pp. 1174–1176, 1975.

[21] C. J. Marriott, J. E. Cadorette, V. Scasner, J. Rousseau, and L. van Lier "High-resolution PET imaging and quantitation of pharmaceutical biodistribution in a small animal using avalanche photodiode detectors," *J. Nucl. Med.,* vol. 35, pp. 1390–1397, 1994.

[22] R. D. Hichwa, "Are animal scanners really necessary for PET," *J. Nucl. Med.,* vol. 35, pp. 1396–1397, 1994.

[23] M. Meyer, C. Anderson, G. Kabalka, and S. Campbell, "Autoradiographic demonstration of magnetic reduction of positron range," *J. Nucl. Med.,* vol. 35, pp. 162P (abstract), 1994.